Iraqi Journal of Physics, 2018 *Vol.16, No.37, PP. 15-22*
DOI: 10.20723/ijp.16.37.15-22

Gas sensing performance of Sol-gel grown NiO-doped Cr_2O_3 nanoparticles

Tunis B. Hassan[1], Abdulkareem M. Ali[2], Ghuson H. Mohammed[1]

[1]Department of Chemistry, College of Science, University of Baghdad, Iraq

[2]Department of Physics, College of Science, University of Baghdad, Iraq

E-mail: tunis20151@gamil.com

Abstract

The sensors based on Nickel oxide doped chromic oxide (NiO: Cr_2O_3) nanoparticals were fabricated using thick-film screen printing of sol-gel grown powders. The structural, morphological investigations were carried out using XRD, AFM, and FESEM. Furthermore, the gas responsivity were evaluated towards the NH_3 and NO_2 gas. The $NiO_{0.10}$: Cr_2O_3 nanoparticles exhibited excellent response of 95 % at 100^oC and better selectivity towards NH_3 with low response and recovery time as compared to pure Cr_2O_3 and can stand as reliable sensor element for NH_3 sensor related applications.

Key words
Sol-gel, gas sensor, NiO doped Cr_2O_3 nanoparticles.

Article info.
Received: Oct. 2017
Accepted: Nov. 2017
Published: Jun. 2018

ادائية المتحسس الغازي لجسيمات اوكسيد الكروم النانوية المطعمة بأوكسيد النيكل المنمى بطريقة المحلول الهلامي

تونس بلاسم حسن[1]، عبد الكريم محمد علي[2]، غصون حميد محمد[1]

[1]قسم الفيزياء، كلية العلوم، جامعة بغداد، العراق

[2]قسم الكيمياء، كلية العلوم، جامعة بغداد

الخلاصة

تم تحضير غشاء سميك من اوكسيد الكروم النقي والمشوب باوكسيد النيكل من الباودر المحضر بتقنية المحلول الهلامي .تم التحقيق من الخصائص التركيبية والمورفولوجية بواسطة حيود الاشعة السينية ومجهر القوى الذرية والماسح الالكتروني. علاوة على ذلك فقد استخدم الغشاء كتطبيق لمتحسس غازي غاز الامونيا وغاز ثاني اوكسيد النتروجين وكانحيث كانت نسبة التشويب 0.10 افضل النسب للاستجابة 98 % لغاز الامونيا عند 100 درجة مئوية أفضل تحسسية نحو NH_3 مع انخفاض وقت الاستجابة والانتعاش بالمقارنة مع Cr_2O_3 النقي ويمكن أن يكون كعنصرمتحسس فعال لتطبيقات المتحسس لغاز NH_3.

Introduction

Metal oxides have wide band gaps because of significant contribution of ionic character to the chemical bonds between the metallic cations and oxide ions. In general, metal oxides are not electrically conducting. However, current interest in material science is in unraveling the fundamental aspects of transparent conducting oxides (TCO) and their applications as semiconducting and conducting transparent thin films. A transparent conducting oxide is a wide band-gap semiconductor that has a relatively high concentration of free electrons in its conduction band. These arise either from defects in the material or from

extrinsic dopants, the impurity levels of which lie near the conduction band edge. As implicit in the name, transparent conductors must be simultaneously transparent and conducting, an unusual combination. The physics behind TCO materials as to why they possess both high conductivity and high transparency is important in attempting to improve our understanding of them and to develop new TCO materials [1]. Metal oxides as nanoparticles can exhibit unique chemical properties due to their limited size and high density of surface atoms [2]. Among metal oxides, special attention has been made on the formation and properties of Cr_2O_3. For nanoparticles of Cr_2O_3, though toxic [3] it can be widely used in fields such as catalyst [4], coating, wear and corrosion resistance [5], advanced colorant [6], H_2 absorption material [7] and so on. It is significant to find an economical process which can be used to prepare them on a large scale.

Experimental procedure

1. Synthesis of pure Cr_2O_3 and NiO doped Cr_2O_3 nanoparticles sensors.

NiO doped Cr_2O_3 nanoparticles were prepared as in the following:
The molar concentration was the same for each [(0.1), Cr $(NO_3)_3.9H_2O$ and Ni $(NO_3)_2.6H_2O$] of the percentages used represented a value (NiO=0.01, 0.06, 0.10). Chromic nitrate, $Cr(NO_3)_3.9H_2O$,$Ni(NO_3)_2.6H_2O$ was dissolved in 50 ml of ethanol and distilled water at room temperature for 1 hour to prepare solution A. 0.5M ,8g of PVA was dissolved in 50 ml of ethanol and distilled water at room temperature for 1 hour to prepare solution B. After that the solution B was added drop wise to solution A with continuous stirring. The mixture was heated to 80 $^{\circ}$C to form a homogeneous sol solution. The obtained sol was slowly heated to evaporate the solvent and it forms a hard homogeneous gel. The Pyrolysis of the final gel was performed at a temperature of 400 $^{\circ}$C for 4 hours. During the pyrolysis process the PVA polymeric network through the outer surface, nickel and chromic nitrate salts simultaneously calcinated and converted into NiO doped Cr_2O_3 nanoparticles. The obtained samples were crushed to prepare a fine powder.

B. Preparation of Films

The mixture of 1g nanoparticles for each (NiO, Cr_2O_3, and doped $NiO_{(0.01,0.06,0.10)}$:Cr_2O_3) in 10 ml acetone was stirred and dispersed by ultrasonic method to give a translucent solution. The homogenous mixture as sensing layer was then screen printed onto its surface and dried at 120°C for three hours using an oven.

2. Characterizations

Recently, nanostructured semiconducting materials were synthesized by different physical and chemical methods. This search represents the various characterization techniques utilized in the present work and it also includes the basic principles of the characterization techniques in X-ray Diffraction (XRD), Atomic Force Microscopy (AFM), field emission scanning electron microscopy **(**FE-SEM).

Results and discussion

1. XRD

The phase identification and structural changes were investigated with the help of X-ray diffraction (XRD) technique. Fig.1 shows the typical XRD patterns recorded 2θ angle range 20-70^{o} for the all synthesized samples. The X-ray analysis of the prepared the thin films was studied according to the prepared method of NiO doped Cr_2O_3, when concentration of NiO (0.01, 0.06, and 0.10) was prepared at room

temperature. Fig. 1 displays X-ray diffraction patterns of the as-prepared Cr_2O_3 and NiO doped Cr_2O_3 samples. The XRD spectra of NiO doped Cr_2O_3 consist of (012) (104), (110), (113), (202), (024), and (116) peaks, and all the observed diffraction peaks can be indexed to Cr_2O_3 rhombohedral structure. The strong (110) peak proves that Cr_2O_3 with rhombohedral structure were obtained in both undoped and NiO doped Cr_2O_3 samples. No diffraction peaks of other structures were detected in these samples, indicating that the NiO ion successfully occupied Cr_2O_3 lattice site and there were no secondary phases or precipitates in the samples. The crystallites sizes of the Cr_2O_3 and NiO doped Cr_2O_3 are estimated using Debye–Scherrer equation.

$$D = \frac{K\lambda}{\beta.\cos\theta} \quad (1)$$

where D is the crystallite size, λ is wavelength of radiation used, β is the full width at the half maximum peak at diffraction angle 2θ.

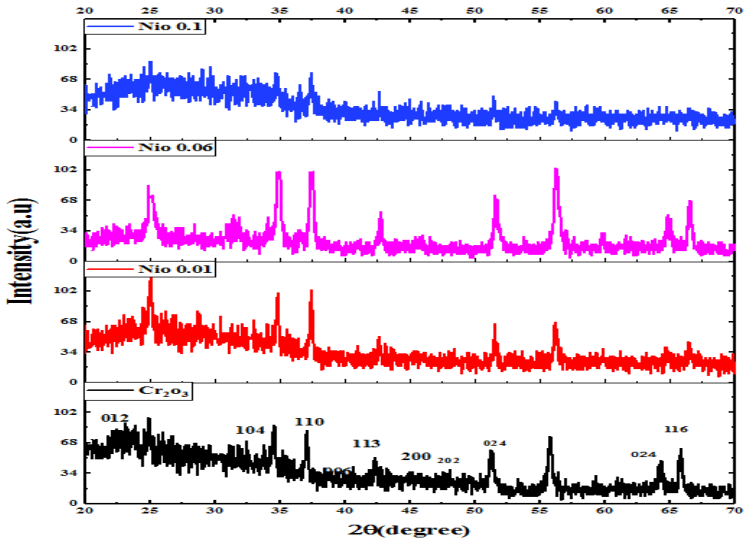

Fig.1: X-ray diffraction pattern of (A) Cr_2O_3 nanoparticles (B)NiO/Cr_2O_3 NPs at 0.01 (C) NiO/Cr_2O_3 NPs at 0.06(D) NiO/Cr_2O_3 NPs at 0.10.

The average values of grain sizes are 25 nm, 24.8 nm, 23.8 nm and 19 nm for the Cr_2O_3, $(Cr_{0.99}Ni_{0.01})$ O_4, $(Cr_{0.94}Ni_{0.06})$ O_4, and $(Cr_{0.90}Ni_{0.10})$ O_4, respectively. The radius of Ni^{2+} was 0.69 Å, which was larger than that of Cr^{3+} (0.62 Å) at the same condition. Therefore, the substitution of Ni^{2+} by Cr^{3+} induced the high angle shift of diffraction peaks, confirming that Ni^{2+} is incorporated into the Cr^{3+} lattice. This indicated that the addition of NiO could effectively prevent Cr_2O_3 crystallites from further growing-up [8].

2. AFM

The AFM image of undoped Cr_2O_3 and doped NiO (0.01, 0.06, and 0.10) nanoparticles in two and three dimensions respectively, is shown in Fig. 2. The results of AFM image for the previous doped and undoped synthesized Cr_2O_3 and NiO nanoparticles showed that the diameter of the particles was average of 59.3 nm and 48 nm receptively. The doped diameter of the particles was average of 74-48 nm respectively.

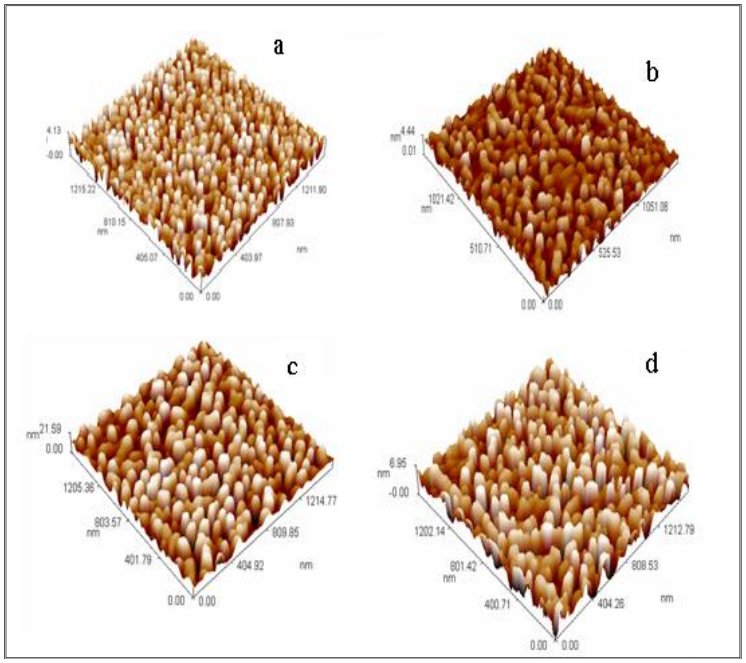

Fig.2: AFM particle size distribution of Cr_2O_3 NPs and NiO (0.01, 0.06, and 0.10).

3. FESEM

The FESEM micrographs of undoped Cr_2O_3 and NiO (0.01, 0.06, and 0.10) doped Cr_2O_3 thin films prepared by print screen at room temperature are shown in Fig.3 a, b,c and d respectively. It can be seen that the pure Cr_2O_3 nanoparticles were nearly uniform spherical shapes and very small particles in evidently dispersed without large agglomerates. Excess addition of NiO into the Cr_2O_3 caused the agglomeration of grains due to the grain growth events. The average diameter of particle 30-60 nm.

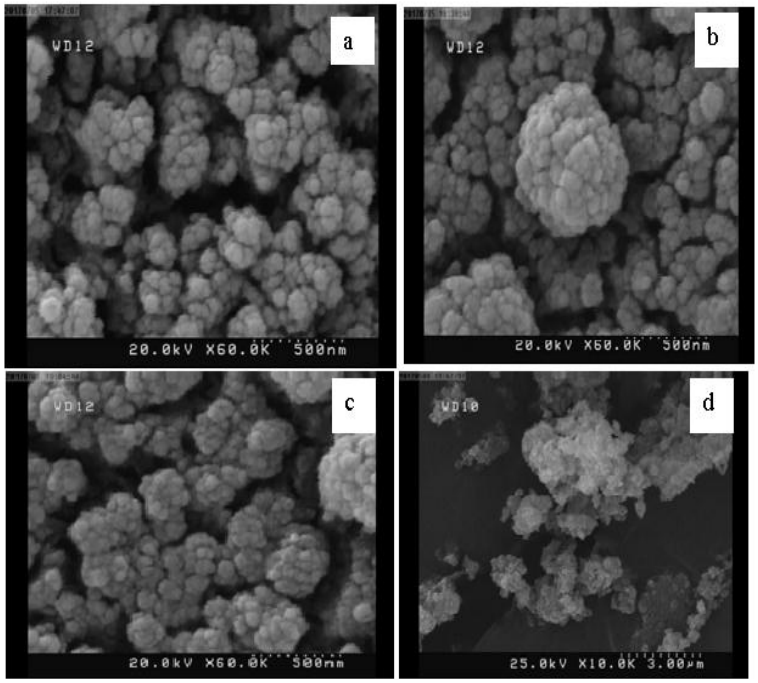

Fig. 3: FESEM image of Cr_2O_3 NPs and doped (A) 0.01(B) 0.06 (C) 0.10.

4. Gas sensing properties

Thin films of Cr_2O_3 and NiO doped Cr_2O_3 nanoparticals were tested to various gases such as: NO_2, NH_3, at operating temperatures ranging from 35 ^oC to 300 ^oC. Fig. 4 shown the relationship between operating temperature and gas response of undoped and NiO doped Cr_2O_3 nanoparticals sensors. The sensor response described in this paper was estimated with the following formula [9]:

$$S= (R_{gas}-R_{air}/R_{air}) \times 100\% \quad (2)$$

where, R_{air} is the resistance in air and R_{gas} is the resistance in presence of test gas at a given temperature. For each sample, the response towards NH_3 increased with operating temperature, reaching its maximum and then decreased rapidly with the increase in operating temperature. Also, it is evident that the response was influenced by Ni addition. This behavior is mainly due to the influence of operating temperature on the amount of absorbed oxygen species on the surface of Cr_2O_3 film [10]. At low temperature, the amount of absorbed oxygen species is low so the sensor response is consequently small while at very high temperature, the progressive desorption of the previously adsorbed oxygen species occurs and, hence, the sensor response decreases. The $NiO_{0.10}$ sample showed maximum response of 95 % toward NH_3 gas at moderate operating temperature of 100ºC which was the highest among all the other samples Cr_2O_3 (22 % at 100 $^\circ C$), $NiO_{0.01}$(58.4 % at 100 $^\circ C$), and $NiO_{0.06}$ (61 % at 100 $^\circ C$) respectively. Smaller crystallite size of $NiO_{0.10}$ sample provides larger specific surface area and higher surface activity for oxygen adsorption. The fast reaction of adsorbed oxygen with ethanol gives a large change in the electrical conductivity of the sensor and eventually a higher sensor response. When the Ni concentration was less than the optimum value the distribution was more discrete and this amount may not be sufficient to promote the reaction effectively whereas for excess Ni there was almost agglomeration of these particles which hinders the reactions. At the optimum concentration (0.10) there was an uniform distribution of these particles as a result of which not only the initial resistance of the sensor is high but this amount can promote the reaction most effectively leading to enhanced response. The fast reaction of adsorbed oxygen with NH_3 gives a large change in the electrical conductivity of the sensor and eventually a higher sensor response.

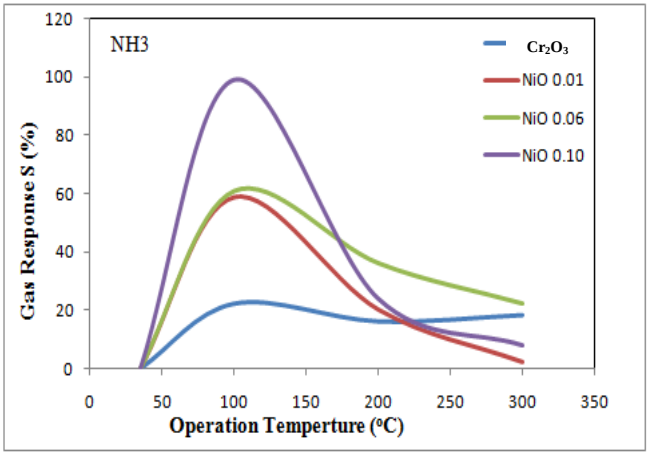

Fig.4: The gas response of NH_3 as a function of operating temperature for undoped and NiO doped Cr_2O_3 nanoparticles.

While in Fig.5 sensing NiO doped Cr_2O_3 the gas NO_2 we observe it will be more responsive. The $NiO_{0.10}$ sample showed maximum response of 43 % at moderate operating temperature of 200 °C, which was the highest among all the other samples Cr_2O_3 (10.5% at 200 °C), $NiO_{0.01}$(20 % at 200 °C), and $NiO_{0.06}$ (27 % at 200 °C) respectively toward the gas NO_2.

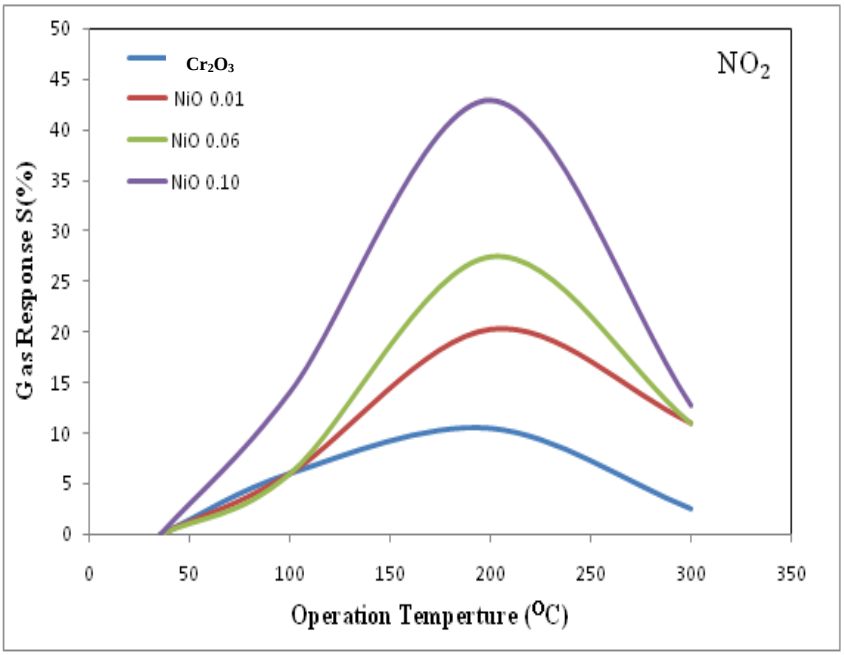

Fig. 5: The gas response of NO_2 as a function of operating temperature for undoped and NiO doped Cr_2O_3 nanoparticles.

The transient response characteristics of all the samples toward the gases NO_2 and NH_3 are shown in Fig.6. These measurements were performed by injecting NO_2 and NH_3 gases into the chamber first and sensors resistance was measured in air and in the presence of NO_2 and NH_3. All the samples respond rapidly as soon as NO_2 and NH_3 gases were injected into the chamber.

Fig. 6 shown the response and recovery times for pure Cr_2O_3 and NiO doped Cr_2O_3 nanoparticles samples. It is seen that the $Ni_{0.10}$ sensor exhibits high selectivity and remarkable response towards NH_3 with response time of 17 s and 41s recovery time, which catalyzes the reaction promoting the rapid electron transfer between the adsorbate and the adsorbent. The sensor resistance rejuvenates to its initial value after purging the NO_2, NH_3 away which indicates the surface of Cr_2O_3 regains the original microstructure after refreshing with carrier gas (air).

In Fig. 7 the relationship between sensitivity and time toward the NH_3 gas was shown.

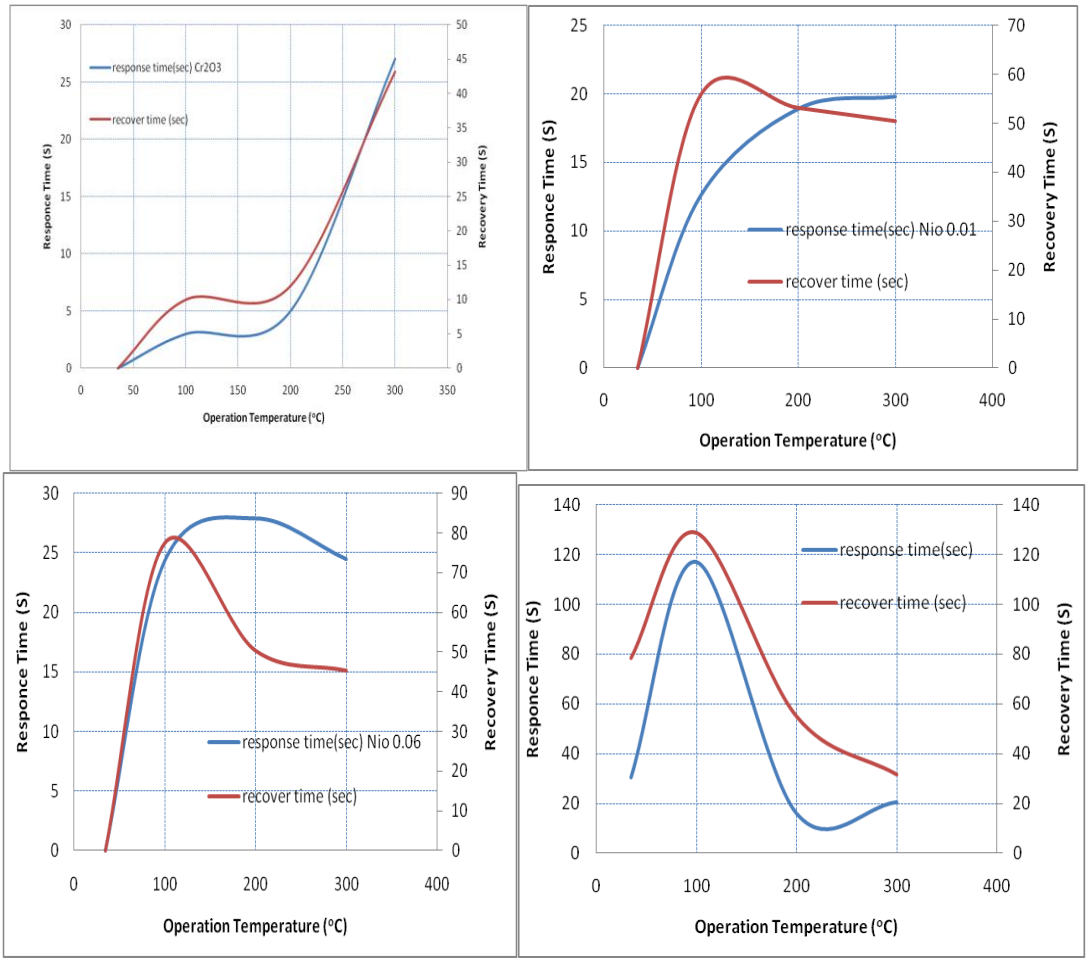

Fig. 6: Response time of the undoped and NiO doped Cr_2O_3 nanoparticles sensor at different working temperatures of NH_3.

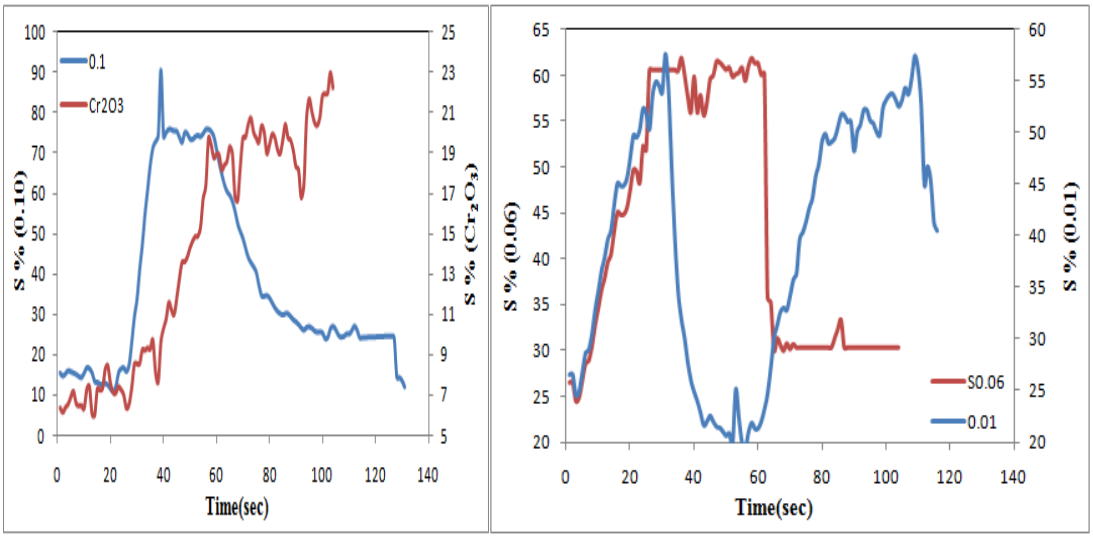

Fig.7: Plots of dynamic response for undoped Cr_2O_3 and NiO-doped Cr_2O_3 nanoparticals samples of NH_3.

Conclusions

Pure Cr_2O_3 and NiO doped Cr_2O_3 nanoparticles film sensors were synthesized by using sol-gel and screen printing routes. XRD studies confirmed the formation of NiO doped Cr_2O_3 nanoparticles materials having crystallite size of 19-25 nm. The

morphological investigations showed the sample surface is fully covered by the spherical grains with average grain size of 30-60 nm. The gas sensing results showed that $NiO_{0.10}$:Cr_2O_3nanoparticals exhibits excellent response (94 %) to NH_3 at 100^oC with fast response (17 s) and recovery time (41 s). The enhanced response is attributed to the smaller crystallite size, which helps in greater oxygen adsorption on the film surface. From transient response and stability study we concluded that $NiO_{0.10}$: Cr_2O_3 nanoparticals can be utilized as a reliable sensor element in NH_3 sensor related applications.

References

[1] Tsoncheva, Tanya, Roggenbuck, Jan Paneva, Daniela Dimitrova, Momtchil Mitov, Ivan, Fröba, Michael, Applied Surface Science, 257 (2010) 523-530.

[2] K. Mohanapandian and A. Krishnan, Adv. Studies Theor. Phys., 8, 6 (2014) 267-276.

[3] Albadarina, B. Ahmad, Al-Muhtaseb, H. Ala'a, Al-laqtah, A. Nasir, Walker, M. Gavin, Allen, J. Stephen, Ahmad, Mohammad N.M., Chemical Engineering Journal (2011) 16920-16930.

[4] Abu-Zied, Bahaa Mohamed, Applied Catalysis A: General, 198 (2000) 139-153.

[5] Pang, Xiaolu, Gao, Kewei, Luo, Fei, Emirov, Yusuf, Levin, Alexandr A., Volinsky, Alex A., Thin Solid Films, 517 (2009) 1922-1927.

[6] Li, Ping, Xu, Hong-Bin, Zhang, Yi, Li, Zuo-Hu, Zheng, Shi-Li,and Bai, Yu-Lan, Dyes and Pigments 80 (2009) 287-291.

[7] R. Vijay, R. Sundaresan, M.P. Maiya, S. Murthy, Srinivasa, Journal of Alloys and Compounds, 424 (2006) 289-293.

[8] Otero-Lorenzo, Ruth, Weber, Mads C., Thomas, Pamela A., Kreisel, Jens, Salgueirin˜o, Vero´nica, Phys. Chem. Chem. Phys., 16 (2014) 22337-22342.

[9] A.M. Soleimanpour, Hou, Yue Jayatissa, H. Ahalapitiya, Applied Surface Science, 257 (2011) 5398-5402.

[10] F. Farzaneh and M. Najafi, Journal of Sciences, Islamic Republic of Iran 22, 4 (2011) 329-333.